A Geometrical Characterization of Regions of Uniqueness and Applications to Discrete Tomography

Paolo Dulio[a,*], Andrea Frosini[b], Silvia M.C. Pagani[a]

[a] *Dipartimento di Matematica "F. Brioschi", Politecnico di Milano, Piazza Leonardo da Vinci* 32, *I*-20133 *Milano*
[b] *Dipartimento di Matematica e Informatica "U. Dini", Università di Firenze, viale Morgagni* 67/*A*, 50134 *Firenze, Italy*

Abstract

In the reconstruction problem of Discrete Tomography, projections are considered from a finite set $\mathcal{S}$ of lattice directions. Employing a limited number of projections implies that the injectivity of the Radon transform is lost, and, in general, images consistent with a given set of projections form a huge class. In order to lower the number of allowed solutions, one usually tries to include in the problem some a priori information. This suggests that modeling the tomographic reconstruction problem as a linear system of equations is preferable.

In this paper we propose to restrict the usual notion of uniqueness, related to the solutions of the linear system, and to provide, for each set $\mathcal{S}$, a geometrical characterization of the shape of a lattice subset, say region of uniqueness (ROU), forming a partial, fast reconstructible, solution.

Any selected set $\mathcal{S}$ intrinsically determines its ROU inside an arbitrary lattice grid. For instance, trivially, if $|\mathcal{S}| = 1$, the ROU is represented by two rectangles having sizes equal to the absolute values of the entries of the unique direction in $\mathcal{S}$, and placed at two opposite corners of the chosen grid. Surprisingly, if $|\mathcal{S}| = 2$, the problem becomes much more complicated.

Our purpose is to provide a geometrical characterization of the ROU. This is based on a double Euclidean division algorithm (DEDA), which runs in polynomial time. It turns out that the ROU is delimited by a zigzag profile obtained by means of numerical relations among the entries of the employed directions. According to different inputs in DEDA, the shape of the ROU can change consistently, as it can be easily observed from the provided examples. Moreover, after selecting a region of interest (ROI) from a given phantom, we exploit DEDA to reconstruct the part of the ROI which falls in the ROU and, with a few further a priori knowledge, even parts of the ROI which are outside the ROU.

2000 *Mathematics Subject Classification.* Primary 94A08; 65R32; Secondary 52C07; 68R; 68U05.

Keywords: Discrete Tomography; Euclidean algorithm; region of interest; region of uniqueness; switching component.

1. Introduction

In *Computerized Tomography* (*CT*) the reconstruction of the density function of an unknown object by means of quantitative data, say projections, collected by incident X-rays, is considered. This can be done

*Corresponding author
Email addresses: paolo.dulio@polimi.it (Paolo Dulio), andrea.frosini@unifi.it (Andrea Frosini), silviamaria.pagani@polimi.it (Silvia M.C. Pagani)

by adapting to the real world situation a theoretical mathematical approach, based on the inversion of the Radon transform. The most significant drawback with a purely theoretical approach relies on the fact that the scan devices allow to collect only a finite number of projections along a fixed set of directions, which implies that there are no chances, in general, of achieving an exact reconstruction by the standard mathematical algorithms. As a matter of fact, the reconstructed object may result quite different from the starting unknown one, sometimes even sharing no elements with it. Moreover, in a medical CT scan analysis, the entire field of view often includes only a region of anatomic interest (ROI). This, on one side, should reduce the needed dose of radiation to be delivered to the patient; from the other side, it prevents the X-rays directions from being arbitrarily chosen, since these must match the requested ROI. In the typical frame of *Discrete Tomography* (DT) [13, 14] only few types of different densities (say, 2-6) are involved, and, in the special case of *Binary Tomography* (BT) we only want to detect the presence or absence of one single material at different parts. The term *discrete* relates both to the change of the domain of the unknown density function into the integer two or three dimensional lattice, i.e., its discretization, and to the fact that the required number of directions, along which projections are taken, is very limited, in order to avoid damaging the objects to be studied. This leads to strong ambiguities in DT reconstructions, and several approaches for a quantitative description of their uncertainty have been already explored (see for instance [10, 23] and the cited bibliography).

1.1. Algebraic approach

Employing a limited number of projections implies that the injectivity of the Radon transform is lost. This suggests a different approach to the (discrete) tomographic reconstruction problem, which can be considered from an algebraic point of view. Here, the density function to be detected, considered as an image consisting of N pixels, is represented as a column vector $\mathbf{x} \in \mathbb{R}^N$. The collected data consist of D different arrays, being D the number of involved directions; the length L_i of the i-th array depends on the corresponding direction. If $M = \sum_{i=1}^{D} L_i$, then a column vector $\mathbf{p} \in \mathbb{R}^M$, representing the whole set of collected measurements, is formed. In this way, the tomographic reconstruction problem is modeled as a linear system

$$W\mathbf{x} = \mathbf{p}, \tag{1}$$

where W is an $M \times N$ matrix, and

$$\sum_{j=1}^{N} w_{ij} x_j = p_i \quad \text{for all } i = 1, ..., M.$$

Reconstructing the image is equivalent to solving the linear system (1).

1.2. Bad configurations

In general, images consistent with a given set of projections form a huge class. Ambiguous reconstructions come out due to the existence of *ghosts*, that is non-zero functions belonging to the null-space of the Radon transform. In the context of DT for finite lattice sets, ghosts are also known under different names, such as *bad configurations* (see for instance [1, 22]), *interchanges*, or *switching components* (this last term has been employed in the literature also in a more general context, see for instance [4, footnote page 2283] for a short comment). More precisely, for a selected set $\mathcal{S}$ of D lattice directions, an $\mathcal{S}$-bad configuration is a pair (Z, W) of lattice subsets of the working grid $\mathcal{A}$, each consisting of K ($\leq 2^{D-1}$) distinct lattice points $z_1, ..., z_K \in Z$ and $w_1, ..., w_K \in W$ such that for each direction $(a, b) \in \mathcal{S}$, and for each $z_j \in Z$, the line through z_j in direction

(a, b) contains a point $w_j \in W$. A region $E \subseteq \mathcal{A}$ admits an $\mathcal{S}$-bad configuration if an $\mathcal{S}$-bad configuration (Z, W) exists for some $D \geq 2$, such that $Z \subseteq E$, $W \subset \mathcal{A} \setminus E$. When the requirement that points in Z or W are distinct is dropped, then we speak about $\mathcal{S}$-*weakly bad configurations*. It becomes apparent that, due to bad configurations, faithful reconstruction of an unknown image is, in general, a hopeless task. Therefore, finding and studying bad or weakly bad configurations is a crucial problem in DT as well as in BT.

1.3. Uniqueness models

Despite the fact that exact reconstructions cannot be achieved in real tomography analysis, applications need theoretical uniqueness models for limited number of projections, in order to have a finite counterpart of the usual integral Radon inversion formula. In order to gain uniqueness, different strategies have been considered, usually relying on additional geometrical or combinatorial information about the unknown image. In particular, one can try to find special sets $\mathcal{S}$ of directions which, jointly with some a priori knowledge, can guarantee uniqueness of reconstruction. For instance, in the class of convex lattice sets, any set $\mathcal{S}$ such that $|\mathcal{S}| \geq 7$ always ensures uniqueness, as well as suitably selected sets of four lattice directions (see [9]).

A different a priori information, which is often considered, is the knowledge of the size of the grid where the object to be reconstructed is confined. In this case, one can take advantage of the algebraic approach introduced by Hajdu and Tijdeman in [12], which allows a polynomial representation of switching components. In [11], this has been exploited to show that uniqueness in a lattice grid can be achieved with four directions satisfying special requests. In [4], this result has been extended to a theoretical uniqueness model for families of four lattice directions (see also [5] for generalization to higher dimensions).

1.4. Local uniqueness

Instead of looking for suitable sets of directions which ensure uniqueness in a whole assigned lattice grid $\mathcal{A}$, one could try to investigate, without prior information, which part of $\mathcal{A}$ can be uniquely reconstructed by means of a set of very few directions, not selected according to some criterion, but arbitrarily given. This idea arises from two different kinds of local approaches to the tomographic reconstruction problem, frequently considered in the literature.

From the one side, the use of particularly suitable directions in real applications could be prevented by some physical or mechanical constraints. It occurs, for instance, in electron microscopy [6], digital breast tomosynthesis [20] or dental tomography [15, 18], where *limited angle reconstructions* based on *truncated sinogram* are exploited.

On the other hand, there may exist situations where an exact reconstruction of the whole image is not necessary, since one might be interested in determining features that are included in some ROI. This is the case of medical CT, when a disease has been previously well-localized and a follow-up scan of the defined region is required.

1.5. Our work

Due to the physics of the scan device and to the highly destructive behavior of the X-rays scan, the number of directions employed in DT is usually extremely low, so linear systems of the form (1) are often underdetermined, and this, in general, makes the related reconstruction problem NP-hard. In this paper, we wish to explore a kind of prior knowledge that could be exploited in the process, in order to extend the class of polynomial-time reconstructible instances: the shape of a region where uniqueness of the reconstruction is guaranteed for a given set $\mathcal{S}$ of directions.

Our proposal is to restrict the usual notion of uniqueness related to the solutions of the linear system, and to provide, for each set $\mathcal{S}$, a geometrical *characterization* of the shape of a lattice subset, say *region of uniqueness* (ROU), forming a partial solution of (1) and that can be fast reconstructed. About that, we start from Definition 1 that gives a natural iterative algorithm to compute the ROU according to the employed directions, and then we show its geometrical counterpart, i.e., an iterative geometrical process to characterize its shape without computing the internal points.

We remark that similar cases often appear in DT, and they usually provide a valuable tool for deeper combinatorial investigations. As an example, when facing the problem of the enumeration of the ROUs related to a given set $\mathcal{S}$ of directions, a geometrical characterization could allow one to define a constructive method to produce all the ROUs according to the growth of one or more parameters, such as semi-perimeter or area. Usually, the idea is to perform local expansions on each element of a certain size and then construct a set of elements of the successive size. Finally, standard techniques, such as Kernel method, appearing in [16], *ECO* method [2], Object Grammars [8] etc. allow us to determine the generating functions of the studied class. A similar construction also leads to an algorithm for the exhaustive generation of the elements of the class. Under some special conditions, this algorithm requires only a constant amount of computation per object, in an amortized sense (algorithms attaining this benchmark are said to have the Constant Amortized Time or CAT property).

Summing up our work, after fixing a sufficiently large lattice grid $\mathcal{A}$, our purpose is twofold.

1. First of all, we aim to characterize the shape of the ROU determined, inside $\mathcal{A}$, by the projections taken in a small set $\mathcal{S}$ of directions for the grid. When $|\mathcal{S}| = 1$, the ROU is trivially represented by two rectangles placed at two opposite corners of $\mathcal{A}$. The size of the rectangles equals the absolute values of the entries of the unique direction in $\mathcal{S}$. Differently, if $|\mathcal{S}| = 2$, the problem becomes much more complicated. Therefore we are interested in providing a complete description of how the ROU can be reconstructed in this case. This is done by means of a double Euclidean division algorithm (DEDA), which requires an amount of time growing polynomially with the components of the directions. It turns out that the ROU is delimited by a zigzag profile obtained by numerical relations among the entries of the pair of employed directions.
2. Secondarily, we focus on how DEDA can be exploited to select in advance pairs of suitable directions that allow a given ROI to be partially, and in some cases completely, included in the ROU. This could be useful in real applications, since one could try to adapt the ROU in order to match some ROI of the image $\mathbf{x}$ to be reconstructed.
   Note that, after computing the projections along pairs of assigned directions, reconstructions can be performed merely by a simple linear time recursive algorithm. Simultaneously, we show the ROU determined by DEDA, pointing out that perfect reconstructions are obtained for any portion of image falling in the ROU. In addition, if we assume to know also the number of different densities, the ROU determined by DEDA can be further enlarged, and a greater portion of the ROI can be determined.

As a qualitative comment we could observe that the NP-hardness of the algebraic approach based on linear system (1) relies in the reconstruction of the *central* portion of the image, while the *border* part, depending on the set $\mathcal{S}$ of employed directions, can be perfectly reconstructed in polynomial time.

Also, it is worth noting that our approach is regardless of the features of the image, such as being binary or with few grey levels.

1.6. Paper organization

The paper is organized as follows. In Section 2 we introduce the basic notations employed in the paper, give the formal definition of the ROU and recall a few preliminary results obtained in [7]. In Section 3, we obtain some general properties concerning the ROU. In Section 4 we show our main results, which lead to the geometrical characterization of the shape of the ROU. We show how the ROU changes according to the slopes of the two considered directions, which deserves a special interest even from the pure combinatorial point of view. It is based on numerical relations among the entries of the employed directions and it is explained by applying a modified version of the Euclidean algorithm (DEDA). Then, in Section 5, we provide a pseudo-code for DEDA, commenting on its complexity. In Section 6 we prove the details about the correctness of the algorithm. This turns out to be the most technical part of the paper. Section 7 is devoted to explicit applications of DEDA. We show the exact reconstruction of the ROU for different choices of the pair of directions (a, b), (c, d). Moreover, we exploit DEDA to reconstruct a ROI included in the ROU and also show how one can profit from some further a priori information to partially extend the ROI outside the ROU. The computations are performed both on phantoms and on real data. Finally, Section 8 gives some perspectives for future works and concludes the paper.

2. Notations and preliminaries

Let $\mathbb{Z}^2$ be the set of points having integer coordinates. We work in a finite rectangular *lattice grid* $\mathcal{A} \subset \mathbb{Z}^2$, having lower-left point in the origin, namely $\mathcal{A} = \{(u, v) \in \mathbb{Z}^2 \mid 0 \leq u < m,\ 0 \leq v < n\}$ for $m, n \in \mathbb{N}$. A point $z \in \mathbb{Z}^2$ can be identified with the unit lattice square having z as lower-left corner, and, in this case, a point is also called *pixel*. We can define a function $f : \mathcal{A} \longrightarrow \mathbb{Z}$, mapping each pixel to an integer value, which corresponds to a color or a grey level of the original image.

Let (a, b) be a discrete direction, i.e., a couple of integers such that $\gcd(a, b) = 1$, with the further assumption that $a = 1$ if $b = 0$ and conversely $b = 1$ if $a = 0$. We say that a finite set $\mathcal{S} = \{(a_j, b_j) \mid j = 1, ..., D\}$ of lattice directions is *valid* for $\mathcal{A}$ if

$$\sum_{j=1}^{D} |a_j| < m, \qquad \sum_{j=1}^{D} |b_j| < n.$$

A *lattice line* is a line containing at least two points in $\mathbb{Z}^2$. The *line sum* of f along the lattice line with equation $ay = bx + t$ is defined as

$$\sum_{av=bu+t,\ (u,v)\in\mathcal{A}} f(u, v).$$

The *projection* of f along the direction (a, b) is the vector whose entries, in a preassigned order, are the line sums of f along all lattice lines with direction (a, b) intersecting $\mathcal{A}$.

Definition 1. A pixel Q is said to be $\mathcal{S}$-geometrically unique (briefly $\mathcal{S}$-unique, or even unique if no confusion arises) if

(a) Q belongs to a line, with direction in $\mathcal{S}$, intersecting the grid just in Q, or

(b) Q lies on a line, with direction in $\mathcal{S}$, whose further intersections with $\mathcal{A}$ are uniquely determined pixels.

The above recursive definition suggests us how to construct the set of $\mathcal{S}$-unique pixels: we first consider pixels falling in case (a), then we recursively extend the uniqueness region including the pixels lying on lines having more than one intersection with the grid.

Definition 2. The *region of uniqueness (ROU)* of $\mathcal{A}$ is the set of pixels of $\mathcal{A}$ that are $\mathcal{S}$-geometrically unique according to Definition 1.

In this paper we are mainly concerned with the determination of the shape of the ROU when $\mathcal{S}$ consists of two distinct valid lattice directions, say (a, b) and (c, d), where we set $a, c < 0$, $b, d > 0$. Basing on these choices, the ROU is constructed by filling the grid $\mathcal{A}$ from its bottom-left corner, and, analogously, from its upper-right corner. Due to symmetry, it suffices to argue only on one of these two regions, say the bottom-left one. Note that our approach is without loss of generality, since, for different choices of the signs of a, b, c, d, the arguments are similar (the ROU just fills different corners of $\mathcal{A}$); in particular, if one of the entries is zero, then the corresponding (coordinate) direction gives no contribution to the determination of the ROU. Moreover, up to transposing the grid and/or changing the order in which directions are taken, we can always assume $-a > b$ and $-a \geq -c$.

In [7], the ROU has been already determined in some particular cases:

- for $b < d$ (see [7, Theorem 2 and Corollary 1]);
- for $b > d$, $\lambda \neq \mu$, being λ, μ the quotients of the division between $-a, -c$ and b, d respectively (see [7, Theorem 3]);
- for $b > d$, $\lambda = \mu$, $0 < r < -c/2$, $s > d/2$, where r, s are the remainders of the above divisions, respectively (see [7, Theorem 4]);
- for $b > d$, $\lambda = \mu$, $r > -c/2$, $0 < s < d/2$ (see [7, Theorem 5]).

The above results show that the ROU consists of displacement of rectangular areas, whose sizes depend on numerical relations among the entries of the employed directions. For instance, the two directions $(-13, 7), (-8, 5)$ produce a ROU as in Figure 1(a). However, the cases treated in [7] seemed to be sporadic examples of a more general picture, which bases on integer division. Our purpose is to complete the characterization of the ROU under two directions.

Denote by $\mathcal{W} = (w_1, w_2, ..., w_{\tau-1}, w_\tau)$ a SE to NW zigzag path, with alternating horizontal and vertical steps of lengths $w_1, w_2, ..., w_{\tau-1}, w_\tau$, being the first one (of length w_1) a vertical step, and the last one (of length w_τ) a horizontal step (see Figure 1(b)).

(a) (b)

Figure 1: (a) The ROU associated to the directions $(-13, 7), (-8, 5)$. (b) The lattice region delimited by the zigzag path $\mathcal{W} = (5, 3, 2, 8, 1, 2)$.

In the case $b < d$, we always obtain the largest possible ROU, which consists of the region delimited by the zigzag path $\mathcal{W} = (b, -a, d, -c)$ (see [7]). From now on we assume that $b \geq d$; in this case, differently from before, we are not sure to gain the largest obtainable area.

3. A few general results

Because of our assumptions, we look for the ROU which is determined in the bottom-left corner of the fixed grid $\mathcal{A}$. Denote by R_0 the $(-a \times b)$-sized rectangle placed in the bottom-left corner of the grid and by R_1, R_1' the two rectangles, of size $-c \times d$, placed, respectively, adjacent to the bottom of the grid and to the right side of R_0, and adjacent to the left side of the grid and to the upper side of R_0 (see Figure 2(a); in what follows, we will not draw the whole grid, but just the configuration in the bottom-left corner).

Theorem 3. The largest obtainable ROU is that delimited by the zigzag path $\mathcal{W} = (d, -c, b-d, -a+c, d, -c)$, i.e., it is the union $R_0 \cup R_1 \cup R_1'$.

Proof. Consider a minimal bad configuration associated to the directions $(a, b), (c, d)$, namely, a parallelogram with sides parallel to the vectors (a, b) and (c, d). We place it such that its highest pixel lies on the left margin of the grid $\mathcal{A}$ and its lowest pixel is placed on the lower side of $\mathcal{A}$. By construction, the pixels of such minimal bad configuration are adjacent to the rectangles R_0, R_1, R_1' (see Figure 2(b)). Our claim is that the pixels on the right and above the bad configuration are not in the ROU. This is evidently true since a bad configuration including one of such pixels is completely contained in $\mathcal{A}$, so its pixels are not uniquely determined. This is equivalent to say that the ROU is contained in the remaining area of $\mathcal{A}$, i.e., in $R_0 \cup R_1 \cup R_1'$. □

Note that all pixels in $\mathcal{R}_0 := R_0 \cup R_1 \cup R_1'$ are uniquely determined, since uniqueness of reconstruction is equivalent to the absence of bad configurations. We say that all pixels in $\mathcal{R}_0$ are *algebraically* unique, as their values are determined by solving the linear system (1).

As one can see from [7], the ROU is in general different from $\mathcal{R}_0$. This is due to the existence of pixels which do not belong to the ROU even if they are not part of a bad configuration contained in the grid $\mathcal{A}$.

Lemma 4. Let $Q \in \mathcal{R}_0$. Then Q is not in the ROU if and only if $Q + z(c, d) \in \mathcal{A} \setminus \mathcal{R}_0$ for some $z \in \mathbb{Z}$ and $Q' + z'(c, d) \in \mathcal{A} \setminus \mathcal{R}_0$ for some $z' \in \mathbb{Z}$, being $Q' = Q + (a, b)$ (or $Q - (a, b)$).

Proof. By the definition of uniquely determined pixel, Q is in the ROU if and only if it is the only unknown in at least one of the equations in the linear system associated to the tomographic problem. There are exactly two equations (namely, two lines) containing Q: one with direction (a, b) and one with direction (c, d). Since in $\mathcal{R}_0$ a line with direction (a, b) has at most two intersections with $\mathcal{A}$, Q belongs to the ROU if and only if Q', if it exists, does so. We then look at the other line through Q, with direction (c, d): Q is in the ROU if and only if there are no other unknowns on that line, namely no intersections with the grid outside the ROU. □

As an example, if $(a, b) = (-6, 5)$ and $(c, d) = (-4, 3)$, we can see that the pixel $Q = (9, 2)$ does not belong to the corresponding ROU. In fact, being $Q' = (9, 2) + (a, b) = (3, 7)$, the translates of Q and Q' by (c, d) (the pixels $(5, 5), (1, 8)$ and $(7, 4), (11, 1)$, respectively) are outside $\mathcal{R}_0$ (see Figure 2(c)).

Remark 5. The previous lemma can be generalized as follows. Suppose to know that the ROU is included in a subset $\mathcal{R}$ of $\mathcal{R}_0$. Then the ROU does not contain a pixel $Q \in \mathcal{R}$ if and only if, for some $z \in \mathbb{Z}$, $Q + z(c, d)$ falls in $\mathcal{A} \setminus \mathcal{R}$, and the same holds also for Q'.

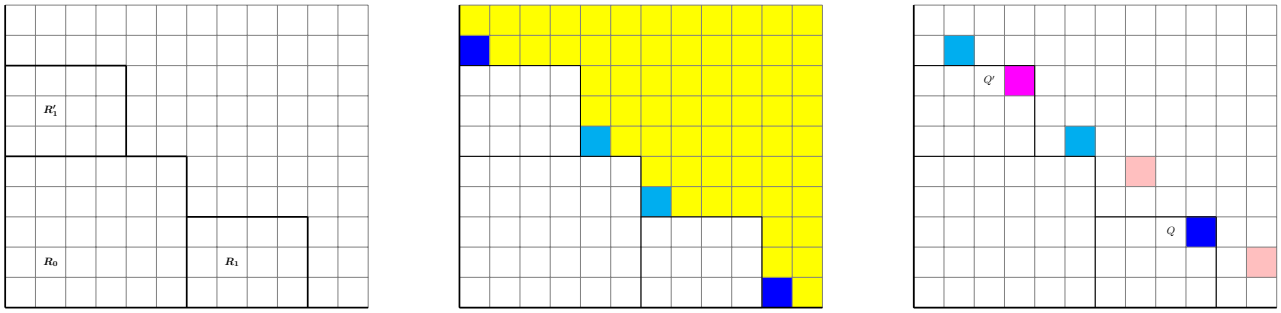

(a) (b) (c)

Figure 2: (a) The displacement of the rectangles R_0, R_1, R'_1, with the directions $(-6, 5)$, and $(-4, 3)$. (b) The displacement of the minimal bad configuration and the removed area (the colored one). (c) The pixels Q, Q' are not in the ROU.

3.1. Comparing algebraic and geometric uniqueness

The set of algebraically unique pixels equals $\mathcal{R}_0$, but the computation of the values of its pixels is NP-hard. On the contrary, the pixel values of the ROU can be obtained, as we will prove later in Section 5.1, in linear time, but the shape of the ROU is not trivial. In the following example, we show that the set of $\mathcal{S}$-geometrically unique pixels differs from the set of algebraically unique pixels. In particular, it results that the ROU is properly included in $\mathcal{R}_0$.

Example 6. Consider an (8×7)-sized grid and the directions $(-4, 3), (-3, 2)$. The corresponding ROU, computed as explained in Section 4, is depicted in Figure 3 (in green). The yellow pixels correspond to $\mathcal{R}_0 \setminus$ ROU. We write the equations involving the undetermined pixels (the first six equations refer to direction $(-4, 3)$, while the other ones to $(-3, 2)$):

$$x_2 + x_8 = b_1, \tag{2}$$
$$x_6 + x_{12} = b_2, \tag{3}$$
$$x_4 + x_{10} = b_3,$$
$$x_3 + x_9 = b_4,$$
$$x_1 + x_7 = b_5,$$
$$x_5 + x_{11} = b_6,$$
$$x_8 + x_{12} + k_1 = b_7, \tag{4}$$
$$x_2 + x_6 + x_{10} = b_8, \tag{5}$$
$$x_4 + x_9 = b_9,$$
$$x_3 + x_7 + x_{11} = b_{10},$$
$$x_1 + x_5 + k_2 = b_{11},$$

where b_is are the projection data and k_1, k_2 are known. If we compute $(2) + (3) - (4) - (5)$, we obtain

$$x_{10} = b_7 + b_8 - b_1 - b_2 - k_1,$$

meaning that x_{10} is uniquely determined, and so are x_3, x_4, x_9.

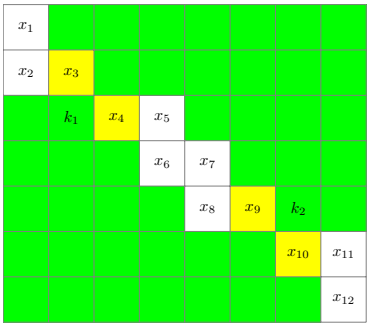

Figure 3: The difference between the geometric ROU (green) and the algebraic ROU (green and yellow).

3.2. Horizontal and vertical convexity of the ROU

Let $\mathcal{B}$ be the minimal bad configuration as in the proof of Theorem 3. The coordinates of the four pixels B_1, B_2, B_3, B_4 of $\mathcal{B}$ are $(0, b+d)$, $(-c, b)$, $(-a, d)$, $(-a-c, 0)$, respectively. Let $\mathcal{B}_j$, $j \in \{1,2,3,4\}$, be the sets of pixels of $\mathcal{A}$ placed in bottom-left region delimited by B_j, namely

$$\begin{aligned}
\mathcal{B}_1 &= \{(0,y) \mid 0 \le y \le b+d-1\},\\
\mathcal{B}_2 &= \{(x,y) \mid 0 \le x \le -c,\ 0 \le y \le b\} \setminus \{(-c,b)\},\\
\mathcal{B}_3 &= \{(x,y) \mid 0 \le x \le -a,\ 0 \le y \le d\} \setminus \{(-a,d)\},\\
\mathcal{B}_4 &= \{(x,0) \mid 0 \le x \le -a-c-1\}.
\end{aligned}$$

Theorem 7. The rectangles $\mathcal{B}_j$, $j \in \{1,2,3,4\}$, belong to the ROU.

Proof. The pixels of $\mathcal{B}_2 \cup \mathcal{B}_3$ are always mapped outside $\mathcal{A}$, when translated along a lattice line parallel to (a,b) or (c,d) (possibly in more than one step, according to Definition 1). Therefore $\mathcal{B}_2 \cup \mathcal{B}_3$ is in the ROU. As concerns the pixels of $\mathcal{B}_1$, these are closer to the bottom side of the grid $\mathcal{A}$ than the pixel B_1. Therefore, when moved on a lattice line along each one of the directions (a,b) and (c,d), they fall either outside $\mathcal{A}$ or in $\mathcal{B}_2 \cup \mathcal{B}_3$, already included in the ROU. Consequently, also $\mathcal{B}_1$ belongs to the ROU. Analogously, the pixels of $\mathcal{B}_4$ are closer to the left side of $\mathcal{A}$ than B_4, and consequently, as above, we can deduce that $\mathcal{B}_4$ is a part of the ROU. □

Corollary 8. The lowest row of the ROU has length $-a-c$ and the leftmost column has height $b+d$.

Proof. It suffices to note that $|\mathcal{B}_1| = b+d$ and $|\mathcal{B}_4| = -a-c$. □

The above results suggest that the ROU is somehow convex. Actually, the ROU determined by a single direction (a,b) is convex, since it is a $(-a \times b)$-sized rectangle: in fact, every line with direction (a,b) containing a pixel of R_0 has no further intersection with the grid. However, for more than two directions a weaker notion of convexity is needed.

Definition 9. A region of a grid is said to be *horizontally* (respectively, *vertically*) *convex* if the intersection of each row (respectively, column) of the grid with the region is a connected set.

In [7, Theorem 6] the ROU determined by a generic set $\mathcal{S}$ of $D \geq 2$ directions, was shown inductively to be horizontally and vertically convex. For the reader's convenience, we give below a new proof which better clarifies our argument.

Theorem 10. The ROU determined by a set $\mathcal{S}$ of directions is horizontally and vertically convex.

Proof. We proceed by induction on the size of the ROU, following its recursive definition. As a preliminary fact, we note that, by Corollary 8, a subset of the lowest row and of the leftmost column of $\mathcal{A}$ are always part of the ROU. This implies that the horizontal and vertical convexity is equivalent to saying that, given a pixel in the ROU, all pixels below it and on its left are part of the ROU.

Consider first

$$\mathrm{ROU}_0 = \bigcup_{j=1}^{4} \mathcal{B}_j,$$

which is horizontally and vertically convex. Then assume the thesis holds for ROU_n, such that $|\mathrm{ROU}_n| = |\mathrm{ROU}_0| + n$, and consider $\mathrm{ROU}_{n+1} = \mathrm{ROU}_n \cup Q$. Since Q is in the ROU, all its shifts along one of the employed directions are in ROU_n. By the inductive argument, all pixels below the shifts of Q belong to the ROU (as they are in ROU_n), and so do also the pixels below Q by a translation along the considered direction (the pixels below Q are the only ones not yet determined on each line).

This proves that the ROU is vertically convex. The proof of the horizontal convexity is analogous. □

4. Algorithmic construction of the ROU

In what follows, we wish to show how the ROU can be determined inside $\mathcal{R}_0$, and, in each case, we characterize its shape. We apply a Double Euclidean Division Algorithm (DEDA), obtained by employing the classical Euclidean division algorithm on the absolute values of the horizontal and, contemporarily, the vertical components ($-a, -c$ and b, d, respectively) of the directions (a, b) and (c, d). This produces two lists of quotients and remainders:

	horizontal		vertical
level 0 :	$-a = h_0(-c) + r_0,$	$b =$	$k_0 d + s_0,$
level 1 :	$-c = h_1 r_0 + r_1,$	$d =$	$k_1 s_0 + s_1,$
level 2 :	$r_0 = h_2 r_1 + r_2,$	$s_0 =$	$k_2 s_1 + s_2,$
$\vdots$	$\vdots$	$\vdots$	

where the two sequences can stop at different levels. In order to compact the notation, we set $-a =: r_{-2}$, $b =: s_{-2}$, $-c =: r_{-1}$, $d =: s_{-1}$. So, at a generic level $j \geq 0$ we have

$$\begin{aligned} r_{j-2} &= h_j r_{j-1} + r_j, \\ s_{j-2} &= k_j s_{j-1} + s_j. \end{aligned}$$

We also set $l_j := \min\{h_j, k_j\}$.

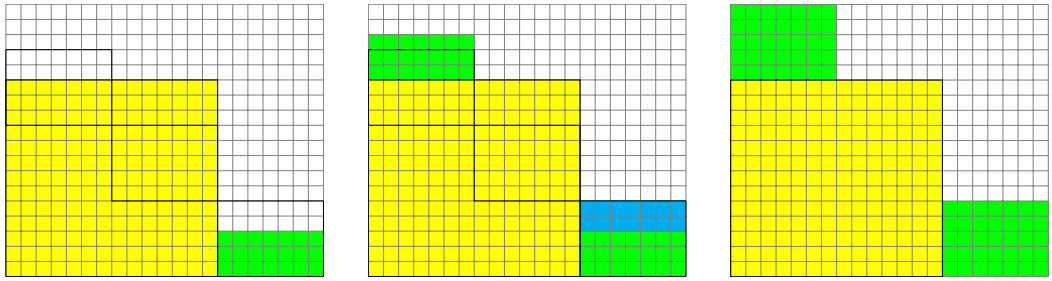

(a) (b) (c)

Figure 4: Construction of the ROU for the directions $(a,b)=(-14,13),(c,d)=(-7,5)$. (a) Only the lowest strip of R_1, of height $s_0=3$, is added, since it is translated inside R_0 along the direction (c,d). (b) By means of a translation along (a,b), a same strip of R_1' is added to the ROU, and then also the remaining part of R_1, by using again (c,d). (c) By means of a translation along (a,b), also the whole rectangle R_1' is part of the ROU.

4.1. The starting level

As a first step, we note that the rectangle R_0, placed in the bottom-left corner of the grid, is always included in the ROU. In fact any of its pixel falls outside $\mathcal{A}$ under a translation by $\pm(a,b)$. We write $\mathcal{R}_j$ for the ROU at step j and consider first the set $\mathcal{R}_0=R_0\cup R_1\cup R_1'$.

Focus on the level 0 as above: if one of the remainders is zero, or the two quotients are not equal, we can argue as follows.

Case 1.1: Suppose $r_0=0$ and note that each line with direction (c,d) through a pixel of the bottom strip of R_1, of height s_0, contains no lattice points outside R_0 and contained in the grid. Consequently, this strip belongs to the ROU. We underline that the length of the strip is precisely $-c$, since $r_0=0$. Now, a same-sized strip in the bottom of R_1' is part of the ROU, by means of the direction (a,b). By iterating the procedure for a finite number of times (since d is finite), we have that the whole rectangles R_1,R_1' are part of the ROU (see Figure 4).

The same argument can be applied for $s_0=0$.

Case 1.2: If $r_0,s_0\neq 0$ and $h_0\neq k_0$, then Theorem 3 of [7] can be applied with $\lambda=h_0$ and $\mu=k_0$. Therefore, as above, we get that the ROU is the largest obtainable one, i.e., it is $\mathcal{R}_0$ (see [7, Example 2]).

Therefore, in the above cases the sets of algebraic uniqueness and geometric uniqueness coincide.

4.2. Erosive procedure

If the two conditions as above are not fulfilled, $\mathcal{R}_0$ undergoes an *erosion*. Since inside $\mathcal{R}_0$ a line with direction (a,b) has at most two intersections with the grid and $R_1+(a,b)=R_1'$, a pixel in R_1 is in the ROU if and only if its translate through (a,b) in R_1' is, so, from now on, we will focus just on R_1 and provide a quick procedure to compute the resulting ROU. Moreover, Theorems 7 and 10 imply that the erosion of the rectangles R_1 and R_1' concerns just their upper-right part.

Inside the rectangle R_1 we can construct a stair-shaped region delimited by blocks having horizontal length r_0 and vertical length s_0. This is what we obtain from level 1 of DEDA.

We have to distinguish two cases.

Case 2.1: The first block is placed on the bottom-right corner of R_1, and its upper-left corner is adjacent to the bottom-right corner of a same-sized block. This one is itself adjacent to another block in its upper-left corner, and so on in order to have $l_1 = \min\{h_1, k_1\}$ blocks (we take the minimum since otherwise the blocks would exceed the rectangle R_1). A residual block of size $r_1 \times s_1$ is added to connect the blocks and the upper-left corner of R_1.

Case 2.2: The same as in Case 2.1, with the only difference that the first block of size $r_0 \times s_0$ is placed on the upper-left corner of R_1 (see subsection 4.3 below for a detailed explanation about how to choose the correct case).

By Theorem 10, erosion regards all pixels above and on the right of each such block, which are consequently removed from $\mathcal{R}_0$. Let $\mathcal{R}_1$ be the resulting region.

By means of the same argument as in the above Cases 1.1 and 1.2, we get that, if r_1 or s_1 is 0, or $h_1 \neq k_1$, then there is no further erosion, and the ROU is $\mathcal{R}_1$. Otherwise, we repeat the procedure by replacing $-c, d$ with r_0, s_0, and r_0, s_0 with r_1, s_1 respectively. As a result, we remove from $\mathcal{R}_1$ the pixels above and on the right of the l_2 $(r_1 \times s_1)$-sized blocks and the $(r_2 \times s_2)$-sized block; we thus obtain $\mathcal{R}_2$ at step 2 of DEDA.

Remark 11. What we said for levels 0 and 1 indeed holds for every level of DEDA. Therefore, while the classical Euclidean algorithm stops when the remainder is zero, DEDA checks whether, at level i,

(a) at least one between r_i and s_i is zero, or

(b) $h_i \neq k_i$

to stop the algorithm.

In a sense, we have that the erodent block becomes the eroded one.

We then iterate the procedure until one of the two conditions of Remark 11 is fulfilled; in this case the algorithm stops, say at step i. In this case, we say that the obtained ROU has *erosive level* i. To better understand what happens when the algorithm stops and which is the form of the last erosion, we refer to Section 4.4.

4.3. How to start the erosion

We want to point out that the choice of *starting from above or from below* in the erosion procedure at level i, i.e., placing the blocks of size $r_{i-1} \times s_{i-1}$ starting from the upper-left corner or the bottom-right one of the rectangle(s) of size $r_{i-2} \times s_{i-2}$ (Cases 2.2 and 2.1, respectively), corresponds to keep, after such an erosion, the largest possible area. In Section 6 we prove that this actually represents the ROU.

Note that the removed area consists of two parts: the *triangular part*, corresponding to the area above (or on the right of) the blocks of size $r_{i-1} \times s_{i-1}$, and the *residual part*, i.e., the pixels above (or on the right of) the remainder block of size $r_i \times s_i$ (see Figure 5). The name "triangular part" derives from the fact that it consists of a triangular number of blocks of size $r_{i-1} \times s_{i-1}$; more precisely, this number is $(l_i - 1)l_i/2$ and it does not change when starting from above or from below. The number of pixels belonging to the triangular part is then

$$\frac{(l_i - 1)l_i}{2} r_{i-1} s_{i-1}.$$

As concerns the residual part, its size is $r_i(s_{i-2} - s_i)$ when starting from above and $s_i(r_{i-2} - r_i)$ when starting from below.

The following lemma holds.

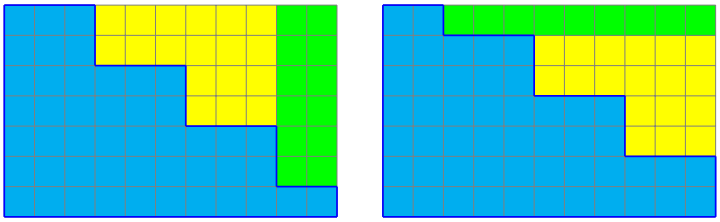

(a) (b)

Figure 5: (a) Starting from above, and (b) starting from below. The triangular part has the same area, while the residual part changes.

Lemma 12. Starting from above (respectively, below) in the erosion of the block $r_{i-2} \times s_{i-2}$, produces a smaller loss of pixels if and only if

$$r_i s_{i-2} - s_i r_{i-2} < 0 \tag{6}$$

(respectively, $r_i s_{i-2} - s_i r_{i-2} > 0$).

Proof. From the previous observations, erosion starts from above if and only if $r_i(s_{i-2} - s_i) < s_i(r_{i-2} - r_i)$, and (6) follows. Analogously, erosion is from below if and only if $r_i s_{i-2} - s_i r_{i-2} > 0$. □

Remark 13. Equality in (6) is not allowed, since this would imply easily (by moving backwards in DEDA), that $-c$ and d are not coprime.

The following theorem ensures that there is no need of verifying at each step which is the start position that maximizes the ROU.

Theorem 14. At step $i+1$, starting erosion from below (respectively, from above) produces the minimal loss of pixels if and only if the erosion at step i is minimized by starting from above (respectively, from below).

Proof. Assume that erosion starts from above at step $i \geq 0$; this means that $r_i s_{i-2} < s_i r_{i-2}$. So, by a simple calculation,

$$\begin{aligned}
(r_{i-2} - l_i r_{i-1}) s_{i-2} &< (s_{i-2} - l_i s_{i-1}) r_{i-2}, \\
r_{i-1} s_{i-2} &> s_{i-1} r_{i-2} \quad (\pm l_i r_{i-1} s_{i-1}), \\
r_{i-1}(s_{i-2} - l_i s_{i-1}) &> s_{i-1}(r_{i-2} - l_i r_{i-1}), \\
r_{i-1} s_i &> s_{i-1} r_i, \\
-l_{i+1} r_{i-1} s_i &< -l_{i+1} s_{i-1} r_i \quad (\pm r_{i-1} s_{i-1}), \\
r_{i-1}(s_{i-1} - l_{i+1} s_i) &< s_{i-1}(r_{i-1} - l_{i+1} r_i), \\
r_{i-1} s_{i+1} &< s_{i-1} r_{i+1},
\end{aligned}$$

which means that erosion at step $i+1$ starts from below. □

Remark 15. The starting point is not calculated at level 0, since this step just gives information about the presence or absence of erosion.

We can summarize the previous considerations by saying that, if i is the erosive level, then, for $j \in \{0, 1, \ldots, i-2\}$, the rectangle $r_j \times s_j$ is eroded by $r_{j+1} \times s_{j+1}$, and the procedure alternates the starts from above and from the below. Moreover, the following result holds.

Corollary 16. The erosion procedure is completely determined by checking whether $r_1 d + s_1 c \lesseqgtr 0$.

Proof. By Theorem 14, the shape of the ROU is completely determined once we know the start of the erosion procedure at level one. By Lemma 12, since $r_{-1} = -c$ and $s_{-1} = d$, this is equivalent to check whether $r_1 d + s_1 c \lesseqgtr 0$. □

In what follows, where not specified, the expression "erosion starts from above (below)" refers to the first erosive level.

4.4. How to obtain the shape of the last eroded block

In this subsection, our purpose is to explain what happens at the last step (say i) of DEDA, namely, when the algorithm stops and the shape of the ROU is obtained. At this step the erosion does not consist of blocks of size $r_{i-1} \times s_{i-1}$ and $r_i \times s_i$, but of slightly different blocks. In fact, the erosion procedure goes on, by alternating starts from above and below, as long as the remainder block is strictly included in the erodent block. When this condition is not satisfied, at least one of the sizes of the remainder block is greater than, or equal to, the size of the corresponding erodent block (see examples in Section 7). This reflects in updating the last line of DEDA according to one of the conditions of Remark 11. More precisely, we proceed as follows.

(a) If one of the remainders is zero, we lower by 1 the corresponding quotient, so that the remainder is updated with the divisor (namely, with the remainder of step $i-1$). For instance, in the case of the horizontal direction, we get $r_{i-2} = (h_i - 1)r_{i-1} + r_{i-1}$. For simplicity, we update the quotient and the remainder:

$$\begin{aligned} h_i &\longleftarrow h_i - 1, \\ r_i &\longleftarrow r_{i-1}. \end{aligned}$$

(b) Once no remainder is zero (possibly without step (a)), we then check the quotients: as previously observed, different quotients imply that one of the sides of the erodent block exceeds the bounding rectangle before the same happens to the other one. So we take $l_i = \min\{h_i, k_i\}$ and rewrite

$$\begin{aligned} r_{i-2} &= l_i r_{i-1} + r_i^*, \\ s_{i-2} &= l_i s_{i-1} + s_i^*; \end{aligned}$$

then the rectangle(s) of size $r_{i-2} \times s_{i-2}$ are eroded by l_i blocks of size $r_{i-1} \times s_{i-1}$, with remainder block of size $r_i^* \times s_i^*$.

We underline that the minimum among the quotients is computed on the updated quotient(s), in the case that one of the remainders is zero (namely, if step (a) occurs). Moreover, note that the case $r_i^* > r_{i-1}$ and $s_i^* > s_{i-1}$ never occurs, since otherwise we could insert an $(r_{i-1} \times s_{i-1})$-sized block into the remainder block. This means that, if $r_i^* > r_{i-1}$ then $s_i^* \leq s_{i-1}$, and, analogously, if $s_i^* > s_{i-1}$ then $r_i^* \leq r_{i-1}$.

We can give now a more detailed description of the stopping criteria of DEDA.

Lemma 17. If DEDA stops at level i, then $r_i^* \geq r_{i-1}$, or $s_i^* \geq s_{i-1}$.

Proof. We know that DEDA stops when one of the remainders among r_i and s_i is zero, or when the quotients h_i and k_i are different. If $r_i = 0$, then $r_i^* \geq r_{i-1}$. Analogously, if $s_i = 0$, then $s_i^* \geq s_{i-1}$. If $h_i \neq k_i$, then we take both quotients equal to $l_i = \min\{h_i, k_i\}$, so that the remainder corresponding to the greater quotient is updated, and one of the previous inequalities is satisfied. □

Theorem 18. Let DEDA stop at level i. Then we have

(*a*) $r_i^* > r_{i-1}$, or $r_i^* = r_{i-1}$ and $s_i^* < s_{i-1}$, if and only if every $(r_{i-2} \times s_{i-2})$-sized block formed by DEDA is eroded from below.

(*b*) $s_i^* > s_{i-1}$, or $s_i^* = s_{i-1}$ and $r_i^* < r_{i-1}$, if and only if every $(r_{i-2} \times s_{i-2})$-sized block formed by DEDA is eroded from above.

Proof. Since DEDA stops at level i, $r_{i-2} \times s_{i-2}$ is the last eroded block. Assume that $r_i^* > r_{i-1}$; then, as observed before, we have $s_i^* \leq s_{i-1}$, since otherwise we could insert an $(r_{i-1} \times s_{i-1})$-sized block into the $(r_i^* \times s_i^*)$-sized block. Therefore we get

$$s_i^*(r_{i-2} - r_i^*) = s_i^* l_i r_{i-1} < s_i^* l_i r_i^* \leq s_{i-1} l_i r_i^* = (s_{i-2} - s_i^*) r_i^*.$$

Consequently, $r_i^* s_{i-2} - s_i^* r_{i-2} > 0$, and, by Lemma 12, this implies that $r_{i-2} \times s_{i-2}$ is eroded from below. Analogously, in case $r_i^* = r_{i-1}$ and $s_i^* < s_{i-1}$, we have

$$s_i^*(r_{i-2} - r_i^*) = s_i^* l_i r_{i-1} = s_i^* l_i r_i^* < s_{i-1} l_i r_i^* = (s_{i-2} - s_i^*) r_i^*,$$

which still implies that erosion is from below. This proves the direct implication.

Conversely, suppose that every $(r_{i-2} \times s_{i-2})$-sized block formed by DEDA is eroded from below. Then, by Lemma 12,

$$s_i^* r_{i-1} < s_{i-1} r_i^*.$$

If $r_i^* > r_{i-1}$, the result follows. Otherwise $s_{i-1} r_i^* \leq s_{i-1} r_{i-1}$, so that $s_i^* < s_{i-1}$. By Lemma 17 this also implies that $r_i^* = r_{i-1}$. This proves (*a*). The proof of (*b*) is analogous. □

Note that the case $r_i^* = r_{i-1}$ and $s_i^* = s_{i-1}$ does not occur, as it would imply that $-c$ and d are not coprime.

4.5. Matching DEDA with previously obtained results

The determination of the ROU for two directions has already been treated in [7], where only some particular cases are studied. Now we want to show how the previous results can be included in these new ones to obtain a unified picture. First, note that the case $b < d$ must be treated separately, since step 0 of DEDA cannot be applied, being the quotient equal to zero. This case has been settled out in [7, Corollary 1] and leads to an L-shaped ROU.

The case $b > d$ was differently explored.

(*a*) Theorem 3 of [7] states that, if the quotients λ, μ (h_0 and k_0 in the present paper) of the division between $-a, -c$ and b, d respectively are not equal, then there is no erosion. This result fits with DEDA, since for $h_0 \neq k_0$ the algorithm stops at step 0 and so the whole rectangles R_1 and R_1' are added to the ROU.

(*b*) In the case $\lambda = \mu$ it is assumed that, for $-a = \lambda(-c) + r_0$ and $b = \mu d + s_0$, r_0 and s_0 are strictly positive numbers. Two different results were found in [7].

(b.1) When $r_0 > -c/2$ and $s_0 < d/2$, at step 1 of the Euclidean algorithm we obtain

$$\begin{aligned} -c &= h_1 r_0 + r_1, \\ d &= k_1 s_0 + s_1, \end{aligned}$$

with $h_1 = 1$ (since $r_0 > -c/2$), $k_1 \geq 2$ (since $s_0 < d/2$). Being $h_1 \neq k_1$, the algorithm stops and the pair of directions has erosive level 1. It means that the rectangle R_1 is eroded by one block of size $r_0 \times s_0$, with remainder block $r_1 \times s_1^*$ (where $s_1^* = d - l_1 s_0 = d - s_0$). Since $-cs_0 < -c\,\frac{d}{2} < r_0 d$, we get $-cs_0 - r_0 d < 0$. Consequently, $-cd - r_0 d < -cs_1^*$, hence $r_1 d + cs_1^* < 0$ and, by Corollary 16, the erosion starts from above. The zigzag profile of the ROU is then $\mathcal{W} = (s_1^*, r_1, s_0, r_0, -a+c, b-d, s_1^*, r_1, s_0, r_0)$, in agreement with the statement of Theorem 4 of [7].

(b.2) The case $r_0 < -c/2$ and $s_0 > d/2$ is obtained analogously, with the only difference that erosion starts from below.

5. A pseudo-code for DEDA

To sum up, DEDA produces the following computations:

$$\begin{array}{lrcl@{\qquad}rcl} & & & \text{horizontal} & & & \text{vertical} \\ \text{level } 0: & -a &=& l_0(-c) + r_0, & b &=& l_0 d + s_0, \\ \text{level } 1: & -c &=& l_1 r_0 + r_1, & d &=& l_1 s_0 + s_1, \\ \text{level } 2: & r_0 &=& l_2 r_1 + r_2, & s_0 &=& l_2 s_1 + s_2, \\ & & \vdots & & & \vdots & \\ \text{level } i: & r_{i-2} &=& l_i r_{i-1} + r_i^*, & s_{i-2} &=& l_i s_{i-1} + s_i^*. \end{array}$$

Algorithm 1 summarizes the above considerations.

In terms of zigzag path, we recall that it consists of a series of horizontal and vertical segments delimiting the ROU, starting from its bottom-right zone. We use the notation $[s, r]^l$ to mean that the block $r \times s$ is repeated l times. So, at step i the path is modified as follows:

$$(s_{i-2}, r_{i-2}) \longmapsto \begin{cases} \left(s_i, r_i, [s_{i-1}, r_{i-1}]^{l_{i+1}}\right) & \text{if starting from above,} \\ \left([s_{i-1}, r_{i-1}]^{l_{i+1}}, s_i, r_i\right) & \text{if starting from below.} \end{cases} \tag{7}$$

Note that at step i only remainders with indices i and $i-1$ appear in the path, as the previous ones are eroded.

In Algorithm 1, we denote by $\mathscr{E}_i$ the set of pixels which are eroded at level i, i.e., during the i-th run of the *repeat* cycle starting at line 12.

5.1. On the computational complexity of DEDA

The computational cost of DEDA can be obtained by analyzing its steps as follows.

- Line 1: the region $\mathcal{R}_0$ is created by updating $O(-a \times b)$ pixels of the grid $\mathcal{A}$;
- lines 2-5: parameters' initialization can be performed in constant time;
- lines 6-8: the output of $\mathcal{R}_0$ requires $O(-a \times b)$ computational time;

Algorithm 1: The Double Euclidean Division Algorithm (DEDA).

Data: $(a,b),(c,d)$: two directions with negative slope.
Result: $\mathcal{R}_i$: the bottom-left part of the ROU under the directions $(a,b),(c,d)$, having erosive level i.
begin

1 $\mathcal{R}_0 \leftarrow R_0 \cup R_1 \cup R'_1$
2 $r_0 \leftarrow -a \bmod -c$
3 $s_0 \leftarrow b \bmod d$
4 $h_0 \leftarrow \frac{-a-r_0}{-c}$
5 $k_0 \leftarrow \frac{b-s_0}{d}$
6 **if** $r_0 s_0 = 0 \vee h_0 \neq k_0$ **then**
7 **print** There is no erosion
8 **return** $\mathcal{R}_0$
else
9 $i \leftarrow 0$
10 $r_{-1} \leftarrow -c$
11 $s_{-1} \leftarrow d$
12 **repeat**
13 $i++$
14 $r_i \leftarrow r_{i-2} \mod r_{i-1}$
15 $s_i \leftarrow s_{i-2} \mod s_{i-1}$
16 $h_i \leftarrow \frac{r_{i-2}-r_i}{r_{i-1}}$
17 $k_i \leftarrow \frac{s_{i-2}-s_i}{s_{i-1}}$
18 **if** $r_i s_i = 0 \vee h_i \neq k_i$ **then**
19 compute r_i^* and s_i^* as in Section 4.4
20 $\mathcal{R}_i \leftarrow \mathcal{R}_{i-1} \backslash \mathscr{O}_i$
until $r_i s_i = 0 \vee h_i \neq k_i$;
21 **return** $\mathcal{R}_i$

- lines 9-11: as lines 2-5;

- lines 12-20: the *while* part performs, at each cycle, a sequence of parameters' updates requiring constant time each (also in the *if* part), and a final ROU update (line 20) that modifies, say erodes, part of the elements of the previously last computed ROU. A simple observation may convince us about the global complexity of these lines: at each step (except the first) at least one pixel is modified, and the number of pixels of the ROU that are modified during the whole *while* run is bounded by the dimension of the ROU itself, i.e., it is again $O(-a \times b)$.

- line 21: again it is performed in $O(-a \times b)$.

Therefore, the final computational complexity of DEDA is $O(-a \times b)$.

A final comment about the complexity of the *while* part of the algorithm is needed. In particular, we want to show the behavior of the worst case of the Euclidean Algorithm in order to give an upper bound to the repetition of the division steps: the result follows from the Lamé Theorem, whose Knuth's version [17] is as follows.

Theorem 19 (G. Lamé, 1845)**.** [1] For $n \geq 1$, let u and v be integers with $u > v > 0$ such that the Euclidean algorithm applied to u and v requires exactly n division steps and such that u is as small as possible satisfying these conditions. Then $u = F_{n+2}$ and $v = F_{n+1}$, where F_k is a Fibonacci number.

Finally, the following result is of our interest.

Corollary 20. If $0 \leq u, v \leq N$, the number of division steps required by the Euclidean algorithm applied to u and v is at most $\lceil \log_\phi(\sqrt{5}N) \rceil - 2$.

Remind that $\phi = \frac{1+\sqrt{5}}{2}$ is the *golden ratio*. It is remarkable that, if we drop the requirement of displaying the ROU area, then the algorithm provides, in at most $O(\log b)$ iterations (assuming that the modulo function takes constant time), a compact form to represent the boundary of the ROU in terms of walks as (7), whose analogy with Lindenmayer's D0L systems (see [21] for definitions and main properties) could be exploited.

6. Consistency of DEDA

From the proof of Lemma 4, we deduce that, in order to show that a pixel Q is in the ROU, we have to consider the line through Q with direction (c, d) and check whether Q is the only not yet determined pixel on that line. To do so, we have to check whether the shifts of Q along (c, d) fall in the previously determined ROU or outside $\mathcal{A}$. If a shift of Q falls in a region which has not been proven to be in the ROU yet, we cannot argue on it. We can say that proving the consistency of DEDA is obtained by adding pixels to the ROU, starting from the rectangle R_0, while DEDA itself acts by removing pixels from the maximal configuration.

As a preliminary case, if DEDA stops at level zero (namely, there is no erosion), consistency has been proven in Section 4. In the remaining cases, consistency is proven in two steps: first, we show that a pixel which is preserved by DEDA actually belongs to the ROU; then, we show that a pixel which is eroded by DEDA is not in the ROU.

[1] Knuth reported that *"this theorem has the historical claim of being the first practical application of the Fibonacci sequence; since then, many others applications of the Fibonacci numbers to algorithms and to the study of algorithms have been discovered"*.

From now on, we sort blocks of size $r_i \times s_i$, inside a block of size $r_{i-1} \times s_{i-1}$, from above to below if erosion at level $i+1$ starts from above, and conversely if erosion starts from below.

6.1. DEDA preserves uniquely determined pixels

We divide the set of preserved pixels into two subsets: the pixels below and on the left of the blocks; and the pixels inside the blocks. For the first subset, we split the proof among the first erosive level and the other ones.

Theorem 21. If erosion starts from above (respectively, below), then every pixel below (respectively, on the left of) the $(r_0 \times s_0)$-sized blocks of R_1 and R'_1 is in the ROU.

Proof. Assume that erosion starts from above and consider the upper rightmost pixel Q below the first $(r_0 \times s_0)$-sized block of R'_1 (see Figure 6(a)); its coordinates are $(r_0 - 1, b + d - s_0 - 1)$. We move it of $-z(c,d)$, $z \in \mathbb{Z}$. For $1 \leq z \leq l_0$, $Q \in R_0$. Its further translation of $-(c,d)$ is

$$Q - (l_0 + 1)(c,d) = (-a - c - 1, -1) \notin \mathcal{A},$$

so Q is the only not-yet-determined pixel on the line with direction (c,d) containing it, then it is part of the ROU. By horizontal and vertical convexity, also all pixels on the left and below Q are in the ROU, and so do their translates along (a,b), which are the pixels below the first $(r_0 \times s_0)$-sized block of R_1.

Consider now the upper rightmost pixel S below the second $(r_0 \times s_0)$-sized block of R'_1; its coordinates are $(2r_0 - 1, b + d - 2s_0 - 1)$ (see Figure 6(a)). For $1 \leq z \leq l_0 - 1$, $S - z(c,d)$ belongs to R_0. A further translation of $-(c,d)$ gives

$$\tilde{S} = S - l_0(c,d) = (-a + r_0 - 1, d - s_0 - 1),$$

meaning that $\tilde{S}$ is the upper rightmost pixel on the left of the first $(r_0 \times s_0)$-sized block of R_1, which is in the ROU by the previous argument. Therefore S is uniquely determined and then in the ROU, and so do all the pixels on its left and below it.

By recursion, we prove that all pixels below the $(r_0 \times s_0)$-sized blocks are in the ROU. If erosion starts from below, the proof is similar. □

In the proof of Theorem 21, the strategy to prove our results is explained: once the upper rightmost pixel Q below the first $(r_0 \times s_0)$-sized block of R'_1 is shown to be in the ROU, so do, by Theorem 10, the pixels on its left and below it, and also the other pixels with the same position as Q with respect to the other $(r_0 \times s_0)$-sized blocks. The pixel Q is the only one, in the set of upper rightmost pixels, falling in the previously determined ROU, while the other ones are moved to another upper rightmost pixel of R_1, so initially we cannot argue on them. If erosion starts from below, Q is placed on the left of the first $(r_0 \times s_0)$-sized block of R_1, ordered from below.

We now want to extend this argument to all erosive levels; to do so, we need the following definition.

Definition 22. If erosion starts from above (respectively, below), a *pivot* at erosive level i is a pixel Q of R'_1 (respectively, R_1), such that:

- if erosion at level i is from above, Q is the upper rightmost pixel below an $(r_{i-1} \times s_{i-1})$-sized block, inside an $(r_{i-2} \times s_{i-2})$-sized block;
- if erosion at level i is from below, Q is the upper rightmost pixel on the left of an $(r_{i-1} \times s_{i-1})$-sized block, inside an $(r_{i-2} \times s_{i-2})$-sized block.

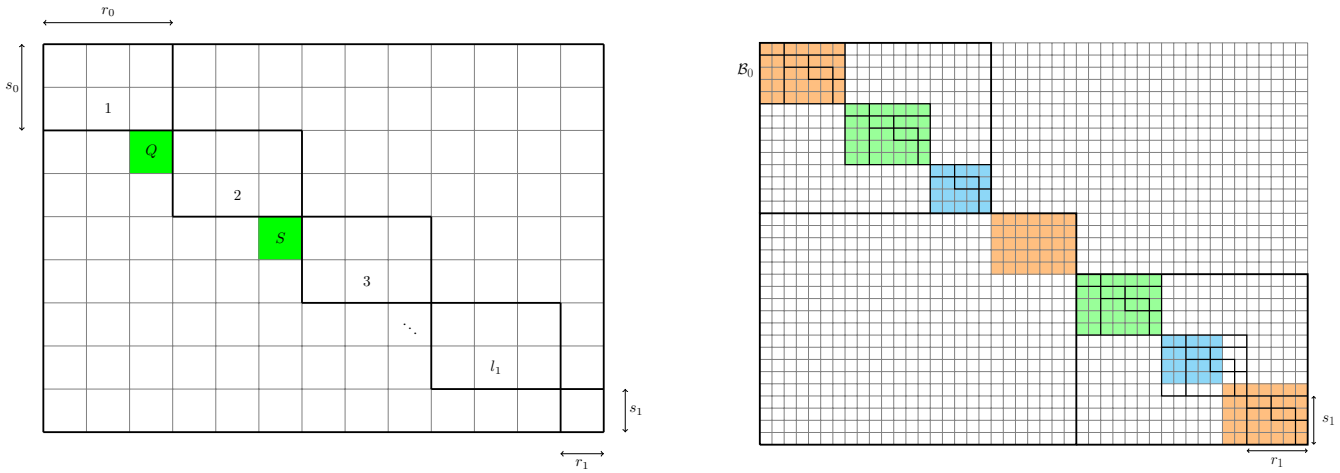

(a) (b)

Figure 6: (a) The position of pixels Q and S in R'_1. (b) The shifts of the $(r_0 \times s_0)$-sized blocks of R'_1.

Lemma 23. Assume erosion starts from above. By translations along the direction (c, d), pivots of R'_1 are moved to pivots of R_1.

Proof. By a translation of $-l_0(c, d)$, the λ-th $(r_0 \times s_0)$-sized block of R'_1, $\lambda = 2, \ldots, l_1$, is moved into the $(\lambda - 1)$-th $(r_0 \times s_0)$-sized block of R_1, so the structure of the pivots inside them does not change.

The first $(r_0 \times s_0)$-sized block of R'_1, say $\mathcal{B}_0$, when moved of $-(l_0 + 1)(c, d)$, is shifted in the lower-right corner of R_1 (see Figure 6(b)). Then, the residual $(r_1 \times s_1)$-sized block of R_1 (at erosive level 1) plays the role of the first (from below) $(r_1 \times s_1)$-sized block in the shift of $\mathcal{B}_0$ (at level 2). This means that the pivot (at level 2) on the left of the first (from below) $(r_1 \times s_1)$-sized block inside $\mathcal{B}_0$ is shifted to the lowest pivot of R_1 (at level 1). Moreover, the pivot (at level 2) on the left of the λ-th $(r_1 \times s_1)$-sized block inside $\mathcal{B}_0$, $\lambda = 2, \ldots, l_2$, is moved to the pivot (at level 2) on the left of the $(\lambda - 1)$-th $(r_1 \times s_1)$-sized block inside the l_1-th $(r_0 \times s_0)$-sized block of R_1.

The residual (at level 1) $(r_1 \times s_1)$-sized block of R'_1 is translated to the upper-right corner of the l_1-th $(r_0 \times s_0)$-sized block of R_1 (see Figure 6(b)). By Theorem 14, the translation preserves the structure of the internal erosion, so the pivot (at level 3) below the first (from above) $(r_2 \times s_2)$-sized block of the residual $(r_1 \times s_1)$-sized block of R'_1 is translated to a pivot of the previous erosive level, while the other pivots fall in other pivots.

As concerns successive erosive levels, the thesis follows from Theorem 14. □

If erosion starts from below, we have to argue on the pivots of R_1; the proof is similar.

As a consequence of the previous lemma, by alternating shifts of $\pm(a, b)$ and $\pm l_0(c, d)$ (or $\pm(l_0 + 1)(c, d)$) all pivots are reached.

Among all pivots at a certain erosive level, there is one that deserves special attention.

Definition 24. The i-th *leading pivot* Q_i is the pixel, among all pivots at erosive level i, such that:

- if erosion starts from above:

- for i even (namely, erosion at level i starts from below), it is the pivot on the left of the first $(r_{i-1} \times s_{i-1})$-sized block, inside the leftmost $(r_{i-2} \times s_{i-2})$-sized block of R'_1:

$$Q_i = (r_{i-2} - r_{i-1} - 1, b + d - s_{i-2} + s_{i-1} - 1);$$

- for i odd (namely, erosion at level i starts from above), it is the pivot above the first $(r_{i-1} \times s_{i-1})$-sized block, inside the rightmost $(r_{i-2} \times s_{i-2})$-sized block of R'_1:

$$Q_i = (-c - r_{i-2} + r_{i-1} - 1, b + s_{i-2} - s_{i-1} - 1);$$

- if erosion starts from below:
  - for i even (namely, erosion at level i starts from above), it is the pivot below the first (from above) $(r_{i-1} \times s_{i-1})$-sized block, inside the rightmost $(r_{i-2} \times s_{i-2})$-sized block of R_1):

$$Q_i = (-a - c - r_{i-2} + r_{i-1} - 1, s_{i-2} - s_{i-1} - 1);$$

  - for i odd (namely, erosion at level i starts from below), it is the pivot on the left of the first (from below) $(r_{i-1} \times s_{i-1})$-sized block, inside the leftmost $(r_{i-2} \times s_{i-2})$-sized block of R_1):

$$Q_i = (-a + r_{i-2} - r_{i-1} - 1, d - s_{i-2} + s_{i-1} - 1).$$

We can say that the leading pivot follows a rule similar to the one exposed in Theorem 14.

In the following result, we show that leading pivots are the pivots which are moved to pivots of the previous erosive level.

Theorem 25. If DEDA stops at level I, then all pixels on the left and below the $(r_{i-1} \times s_{i-1})$-sized blocks of R_1 and R'_1, $i = 1, \ldots, I$, are in the ROU.

Proof. Assume that erosion starts from above. Denote by Q_i the leading pivot of R'_1 at erosive level i. We prove by induction on $i \geq 1$ that Q_i is $\mathcal{S}$-geometrically unique.

For $i = 1$, the result has been proven by Theorem 21.

Assume now that the thesis holds at a level $i \geq 1$; we want to show that the area below the configuration at level $i + 1$ is in the ROU. Assume that i is odd; the coordinates of the leading pivot at level $i + 1$ are

$$Q_{i+1} = (r_{i-1} - r_i - 1, b + d - s_{i-1} + s_i - 1).$$

Being $i + 1$ even, erosion at level $i + 1$ starts from below and Q_{i+1} is in the leftmost $(r_{i-1} \times s_{i-1})$-sized block, so its shifts of $-z(c, d)$, $z \in \{1, \ldots, l_0\}$, remain inside R_0. A further shift gives

$$Q_{i+1} - (l_0 + 1)(c, d) = (-a - c - r_0 + r_{i-1} - r_i - 1, s_0 - s_{i-1} + s_i - 1).$$

As concerns the first component, we can rewrite the terms $-c$ and $-r_0$ as follows:

$$-c = l_1 r_0 + r_1 = l_1 r_0 + l_3 r_2 + r_3 = \ldots = \sum_{j=0}^{\frac{i-1}{2}} l_{2j+1} r_{2j} + r_i$$

and

$$-r_0 = -l_2 r_1 - r_2 = -l_2 r_1 - l_4 r_3 - r_4 = \ldots = -\sum_{j=1}^{\frac{i-1}{2}} l_{2j} r_{2j-1} - r_{i-1}.$$

Then the first component of $Q_{i+1} - (l_0+1)(c,d)$ is then

$$-a + l_1 r_0 - l_2 r_1 + \ldots + l_i r_{i-1} - l_{i-1} r_{i-2} - 1.$$

An analogous argument on the second coordinate gives us

$$d - l_1 s_0 + l_2 s_1 + \ldots - l_i s_{i-1} + l_{i-1} s_{i-2} - 1,$$

meaning that $Q_{i+1} - (l_0+1)(c,d)$ is placed in the l_1-th $(r_0 \times s_0)$-sized block of R_1, in its l_2-th $(r_1 \times s_1)$-sized block, in its l_3-th $(r_2 \times s_2)$-sized block, ..., in the upper rightmost position under its l_i-th $(r_{i-1} \times s_{i-1})$-sized block, namely, by the induction, in the ROU which was determined at the previous step. So, as in the proof of Theorem 21, all pixels below and on the left of Q_{i+1} are in the ROU, and so do all other pivots of level $i+1$, by Lemma 23, and the pixels below them and on their left. This means that all pixels below the configuration at level $i+1$ belong to the ROU.

If i is even, the proof is similar (up to moving Q_{i+1} of $-l_0(c,d)$ instead of $-(l_0+1)(c,d)$). If erosion starts from below, the proof is similar. □

Theorem 26. If DEDA stops at level i, then the pixels inside the $(r_{i-1} \times s_{i-1})$-sized blocks and the residual $(r_i^* \times s_i^*)$-sized block are part of the ROU.

Proof. Assume first that erosion starts from above and stops at level one. By Theorem 18, there are three possible situations: when $s_1^* > s_0$ and $r_1^* = r_0$; when $s_1^* > s_0$ and $r_1^* < r_0$; and when $s_1^* = s_0$ and $r_1^* < r_0$.

In the first case, let Q be the lower rightmost pixel inside the residual $(r_1^* \times s_1^*)$-sized block of R_1, namely $Q = (-a-c-1, 0)$. By Theorem 7, the lowest row of the configuration is known to belong to the ROU, as well as the leftmost column. The line through Q with direction (c,d) intersects the grid in R_0 and in

$$Q + (l_0+1)(c,d) = (r_0 - 1, b + d - s_0),$$

which is the lower rightmost pixel in the first $(r_0 \times s_0)$-sized block of R_1', and therefore is added to the ROU, as well as all pixels in the lowest strip of such block, by horizontal convexity. Then, by alternating shifts of $-(a,b)$ and $+l_0(c,d)$, all the lowest strips of the blocks of size $r_0 \times s_0$ and $r_1^* \times s_1^*$ are added to the ROU. The last added strip is the one inside the l_1-th $(r_0 \times s_0)$-sized block of R_1, whose rightmost pixel's coordinates are $(-a + l_1 r_0 - 1, s_1^*)$. If we move this pixel along (c,d), we obtain

$$\begin{aligned} \tilde{Q} &= (-a + l_1 r_0 - 1, s_1^*) + l_0(c,d) \\ &= ((l_1+1) r_0 - 1, b - s_0 + s_1^*) \\ &= (l_1 r_0 + r_1^* - 1, b - s_0 + s_1^*) \\ &= (-c - 1, b - s_0 + s_1^*), \end{aligned}$$

which is the rightmost pixel of a certain strip of the residual $(r_1^* \times s_1^*)$-sized block of R_1' (not the lowest one, since $s_1^* > s_0$). This means that $\tilde{Q}$ is part of the ROU, as well as the pixels on its left and below it. Also, so do their shifts by $-(a,b)$ in R_1. By going on adding strips, we fill all blocks.

If $s_1^* > s_0$ and $r_1^* < r_0$, the previous argument works similarly; the only change consists in the fact that, being $r_1^* < r_0$, the lowest strip of the l_1-th sized block of R_1 is not completely included in the residual block of R_1', when moved of $l_0(c,d)$. In this case, we consider just the part of the strip falling in the $(r_1^* \times s_1^*)$-sized block and discard the remaining part.

For $s_1^* = s_0$ and $r_1^* < r_0$, we argue as before, but by adding vertical strips.

If erosion starts from below, the proof is similar.

If erosion does not stop at level one, our argument starts again from the lower rightmost pixel of R_1. The thesis follows from the proof of Theorem 25, since the lower rightmost pixel of each block of size $r_{i-1} \times s_{i-1}$ or $r_i^* \times s_i^*$ is obtained by a pivot by a translation of $+(0,1)$. □

6.2. Pixels deleted by DEDA are not uniquely determined

We now prove that pixels which are eroded by DEDA are not part of the ROU.

Theorem 27. Assume that DEDA stops at level one. Then all pixels which are removed by DEDA are not in the ROU.

Proof. Assume that erosion starts from above and consider the pixels in R_1', on the right of the first $(r_0 \times s_0)$-sized block. Let Q_1 be the lower leftmost of such pixels; its coordinates are $(r_0, b+d-s_0)$. We shift it l_0 times in direction (c,d):

$$Q_1 - l_0(c,d) = (-a,d) \notin \mathcal{R}_0,$$

so Q_1 is not the only unknown on that line. To show that Q_1 is not uniquely determined, we have to prove that also $Q_2 = Q_1 - (a,b)$ is not uniquely determined.

When moved of $l_0(c,d)$, Q_2 is sent to the lower leftmost pixel on the right of the second $(r_0 \times s_0)$-sized block of R_1', say Q_3. This means that

$$Q_1 \notin \text{ROU} \iff Q_2 \notin \text{ROU} \iff Q_3 \notin \text{ROU}.$$

Set $Q_4 = Q_3 - (a,b)$; when translated of $l_0(c,d)$, it falls in the lower leftmost pixel on the right of the third $(r_0 \times s_0)$-sized block of R_1'. By iterating the argument, we obtain that

$$Q_1 \notin \text{ROU} \iff Q_2 \notin \text{ROU} \iff \ldots \iff Q_{2l_1} \notin \text{ROU}, \tag{8}$$

where $Q_{2l_1} = (-a + l_1 r_0, d - l_1 s_0)$ is the lower leftmost pixel on the right of the l_1-th $(r_0 \times s_0)$-sized block of R_1, and above the residual $(r_1 \times s_1)$-sized block. Then

$$Q_{2l_1} + l_0(c,d) = ((l_1+1)r_0, b - s_0 + s_1)\,.$$

Since erosion starts from above and stops at level one, by Theorem 18 $s_1 = s_1^* \geq s_0$, so $b - s_0 + s_1 \geq b$ and then $Q_{2l_1} + l_0(c,d) \notin \mathcal{R}_0$. By (8), all the lower leftmost pixels on the right of the $(r_0 \times s_0)$-sized blocks are not uniquely determined, and therefore not in the ROU. By convexity, also pixels over them and on their right are not part of the ROU.

If erosion starts from below, the proof is similar. □

We now move to the general case. Here, we call *pivot* the lower leftmost pixels on the right of (or above, depending on the starting of the erosion) the blocks. The *leading pivot* is the pixel we have to consider to prove our results.

Theorem 28. If erosion stops at level i, then all pixels on the right and above the blocks of size $r_{i-1} \times s_{i-1}$ and $r_i^* \times s_i^*$ do not belong to the ROU.

Proof. It suffices to note that the leading pivot Q at level i is the pivot of the proof of Theorem 25, moved of $+(1,1)$. The argument on that proof showed that the pivot is moved to a previously determined pixel, and then Q is moved into the lower leftmost pixel of $\mathscr{E}_{i-1}$, namely into the area which was eroded by DEDA at level $i-1$. The thesis follows from Remark 5. □

Theorems 25, 26 and 28 together ensure the consistency of DEDA.

7. Experimental results

We now apply DEDA to different experiments. First of all we describe explicitly each step involved in determining the ROU for some assigned sets $\mathcal{S}$ of pairs of lattice directions. The resulting shape of the ROU is shown. Then we apply DEDA in combination with a simple deterministic reconstruction algorithm, in order to investigate particular regions of interest.

7.1. Reconstruction of the shape of the ROU with DEDA

Example 29. Consider $(a,b) = (-13, 11)$ and $(c,d) = (-8, 7)$. We get

			horizontal			vertical
level 0 :	13	=	$1 \cdot 8 + 5$,	11	=	$1 \cdot 7 + 4$,
level 1 :	8	=	$1 \cdot 5 + 3$,	7	=	$1 \cdot 4 + 3$,
level 2 :	5	=	$1 \cdot 3 + 2$,	4	=	$1 \cdot 3 + 1$,
level 3 :	3	=	$1 \cdot 2 + 1$,	3	=	$3 \cdot 1 + 0$.

The algorithm stops al level 3, since one of the remainders is zero. We lessen the quotient and rewrite the last line:

$$\text{level } 3: \; 3 = 1 \cdot 2 + 1, \qquad 3 = 2 \cdot 1 + 1;$$

the quotients are not equal, so the last line becomes

$$\text{level } 3: \; 3 = 1 \cdot 2 + 1, \qquad 3 = 1 \cdot 1 + 2.$$

Figure 7 shows the evolution of the erosive profile; note that, since $r_1 d + s_1 c = 3 \cdot 7 - 3 \cdot 8 < 0$, then the erosive block $r_0 \times s_0$ (5×4 in this case) is placed in the upper-left corner of R_1, i.e, erosion starts from above.

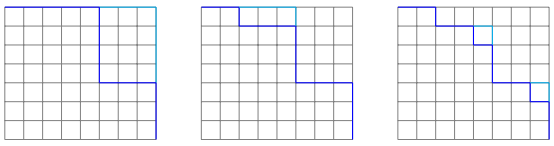

(a) (b) (c)

Figure 7: The three pictures represent the erosion of the rectangle R_1 for the directions $(-13, 11), (-8, 7)$. (a) Erosive profile at level 1 ($\mathcal{R}_1$). (b) Erosive profile at level 2 ($\mathcal{R}_2$). (c) Erosive profile at level 3 ($\mathcal{R}_3$).

Example 30. Consider the directions $(a, b) = (-36, 29)$, $(c, d) = (-26, 21)$. By applying DEDA we get:

$$\begin{array}{lrcl|rcl} & & & \text{horizontal} & & & \text{vertical} \\ \text{level } 0: & 36 & = & 1 \cdot 26 + 10, & 29 & = & 1 \cdot 21 + 8, \\ \text{level } 1: & 26 & = & 2 \cdot 10 + 6, & 21 & = & 2 \cdot 8 + 5, \\ \text{level } 2: & 10 & = & 1 \cdot 6 + 4, & 8 & = & 1 \cdot 5 + 3, \\ \text{level } 3: & 6 & = & 1 \cdot 4 + 2, & 5 & = & 1 \cdot 3 + 2, \\ \text{level } 4: & 4 & = & 2 \cdot 2 + 0, & 3 & = & 1 \cdot 2 + 1. \end{array}$$

At level 4 the algorithm stops, since the remainder in the horizontal direction is zero. The last line is rewritten as follows:

$$\text{level } 4: \quad 4 = 1 \cdot 2 + 2, \qquad 3 = 1 \cdot 2 + 1. \tag{9}$$

The quotients are equal, so $l_4 = 1$ and (9) tells us that the block 4×3 is eroded by one block 2×2 with remainder block 2×1. Since $r_1 d + s_1 c = 6 \cdot 21 - 5 \cdot 26 = -4 < 0$, erosion at level 1 starts from above (see Figure 8(a)).

Example 31. Consider now the couple of directions $(a, b) = (-25, 17)$, $(c, d) = (-11, 7)$. DEDA produces the following calculations:

$$\begin{array}{lrcl|rcl} & & & \text{horizontal} & & & \text{vertical} \\ \text{level } 0: & 25 & = & 2 \cdot 11 + 3, & 17 & = & 2 \cdot 7 + 3, \\ \text{level } 1: & 11 & = & 3 \cdot 3 + 2, & 7 & = & 2 \cdot 3 + 1. \end{array}$$

At level 1 the two quotients are not equal, so DEDA stops. We then rewrite level 1:

$$\begin{array}{lrcl|rcl} & & & \text{horizontal} & & & \text{vertical} \\ \text{level } 1: & 11 & = & 2 \cdot 3 + 5, & 7 & = & 2 \cdot 3 + 1; \end{array}$$

the erosion of the rectangle R_1 is represented in Figure 8(b). Erosion starts from below, since $r_1 d + s_1 c = 3 > 0$.

(a) (b)

Figure 8: The shape of the ROU determined by DEDA for two different pairs of directions (only the rectangle R_1 is drawn). (a) The ROU for the directions $(-36, 29), (-26, 21)$. (b) The ROU for the directions $(-25, 17), (-11, 7)$.

7.2. Matching DEDA with the reconstruction of a ROI

Besides the benefit DEDA offers in a combinatorial perspective, it can be also employed to actually match a ROU with regions of interest which are included in previously scanned images. More precisely, once a ROI has been detected, one can exploit DEDA to find pairs of directions whose corresponding ROU contains the ROI. Then the ROI can be easily reconstructed in polynomial time, with respect to its dimension, by iteratively scanning the ROU area and keeping track of the number of not-yet-unique pixels on each line. When a pixel

is the only one remaining on a line, it becomes unique and is added to the ROU. This deterministic strategy, that resembles the definition of ROU, reveals very useful, mainly when the ROI belongs to the boundary of the scanned image, since it can be more easily included in a ROU for some pair of directions. Consequently, the closer the ROI is to the boundary of the grid, the better the reconstruction algorithm performs. Since the boundary of the grid is a direction-dependent concept, it can be small or large according to the choice of the set $\mathcal{S}$ of projection. This shows the usefulness of DEDA in pre-selecting pairs of directions which can be employed in a reconstruction process.

In this same fashion, some reconstruction algorithms, such as the one proposed in [1], which are related to the recovery of *hv-convex polyominoes* by using horizontal and vertical projections, make some guesses about the positions of the points belonging to the border or to specific areas of the minimal bounding rectangle of the unknown set. Such a strategy highly increases the computational complexity of the process, and could be avoided by including the points of interest inside the ROU (computed by DEDA) of two further suitable chosen directions, in a preprocessing stage.

Remark 32. Combining DEDA with a set of projection data, the number of different grey levels included in the ROU can be also deduced. This could be assumed as an estimate of the number of grey levels in the whole picture, and exploited in some typical reconstruction algorithm, such as DART, where this information is commonly introduced as an a priori assumption, even if no strategy is usually outlined on how to get such a required knowledge. Actually, in [3] the authors proposed the *Discrete Grey Level Selection* approach (DGLS). The presented algorithm estimates a single grey level at a time, assuming as the input, along with the projection data, also a suitable ROI selected by the user, called *user-selected part* (USP). After selecting the USP, an optimization algorithm is used to minimize a grey level penalty function. However, this approach could be computationally expensive, and, also, it cannot be used when the object has a complex topology, without sufficiently large homogeneous regions. Recently, a novel approach has been introduced for the tomographic reconstruction of binary images (see [19]), where, when the two grey levels are unknown, their mid-level value is iteratively approximated during the optimization process. In our proposal the pre-determination of the ROU allows a linear time estimation of the number of grey levels in the ROI (exact estimation if the ROI is completely included in the ROU), so it might be preferable in some applications.

Below we show a few experimental results concerning the search of a suitable ROU including special regions of interest, and their subsequent reconstructions in linear time with respect to the size of the ROU. Three different pairs of directions have been employed, namely $\{(-14,13),(-7,5)\}$, $\{(-36,29),(-26,21)\}$, $\{(-22,45),(-18,37)\}$, respectively (note that in the last case it results $-a < b$ and DEDA works anyway). Results are shown in the figures below; all outputs are plotted by MATLAB. We point out that different pairs of directions lead to a ROU which includes different particulars of the ROI; in some cases, the whole ROI is determined.

First of all we have focused on a brain phantom consisting of 50 different grey levels. A rectangular ROI has been selected in the original image, and different pairs of directions have been considered, in order to try to include in the ROU determined by DEDA an increasing portion of (possibly all) the ROI. Then an easy reconstruction algorithm, running in linear time, has been applied (see Figure 9). Note that some points of the phantom are reconstructed even outside the ROU. This is obtained by adding to DEDA the extra information that the number of employed grey levels is estimated by the number of grey levels included in the ROU (see Remark 32). For instance, if the projection results zero on a line with more than one intersection with $\mathcal{A} \setminus \mathcal{R}_i$, we know that all pixels on that line are zero. This activates an iterative procedure which possibly allows to gain several further pixels not included in the ROU.

As further applications we have explored, for different pairs of directions, the improvements in the reconstruction of a ROI in a slice of the human head at the Atlas cervical vertebra level (Figure 10), as well as a ROI included in the Atlas itself (Figure 11).

Figure 9: (a) The brain phantom (the ROI is the area inside the red triangle). (b) The ROU for the pair $(-14, 13), (-7, 5)$. (c) The ROU for the pair $(-36, 29), (-26, 21)$. (d) The ROU for the pair $(-22, 45), (-18, 37)$.

8. Conclusions

In this paper we have considered the tomographic problem of characterizing the region of uniqueness associated to X-ray data collected along two valid arbitrarily assigned directions for a given lattice grid. We provided the theoretical results which explain how the ROU can be reconstructed from the entries of the X-ray directions, leading to a complete determination of the shape of the ROU. It turns out that the ROU consist of rectangular subregions determined by numerical relations among the entries of the directions. Such a characterization is obtained by means of a polynomial time algorithm based on a double Euclidean division algorithm (DEDA). This reflects in providing an a priori knowledge of which directions could be selected in order to match the ROU with a given ROI.

From an applicative point of view, this is useful, since the reconstruction process inside the ROU runs in polynomial time, or even linear time, simply by employing a deterministic algorithm. We have shown how DEDA can be exploited in matching regions of interest selected in a given phantoms.

Combining DEDA with a set of projection data, the number of different grey levels included in the ROU can be also deduced. This could be assumed as an estimate of the number of grey levels in the whole picture, and exploited in some typical reconstruction algorithm, such as DART, where this information is commonly introduced as an a priori assumption.

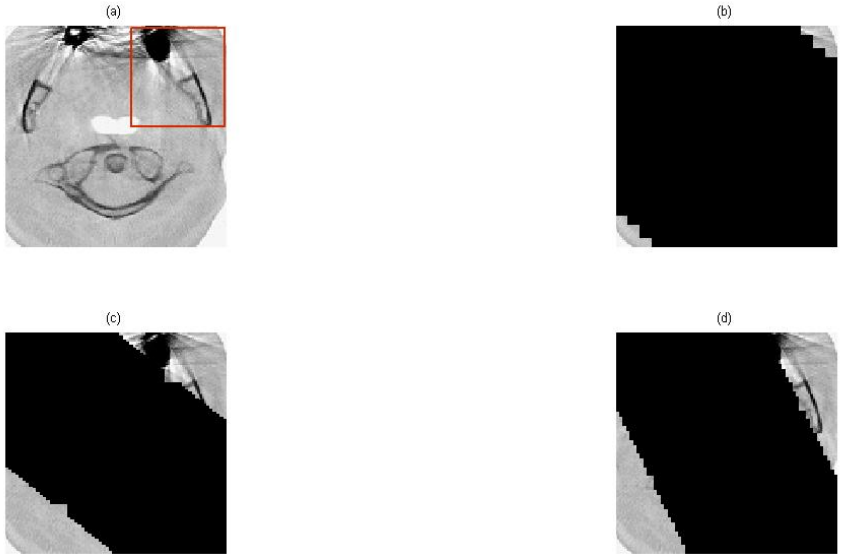

Figure 10: (a) The head phantom (the ROI is the area inside the red rectangle). (b) The ROU for the pair $(-14, 13), (-7, 5)$. (c) The ROU for the pair $(-36, 29), (-26, 21)$. (d) The ROU for the pair $(-22, 45), (-18, 37)$.

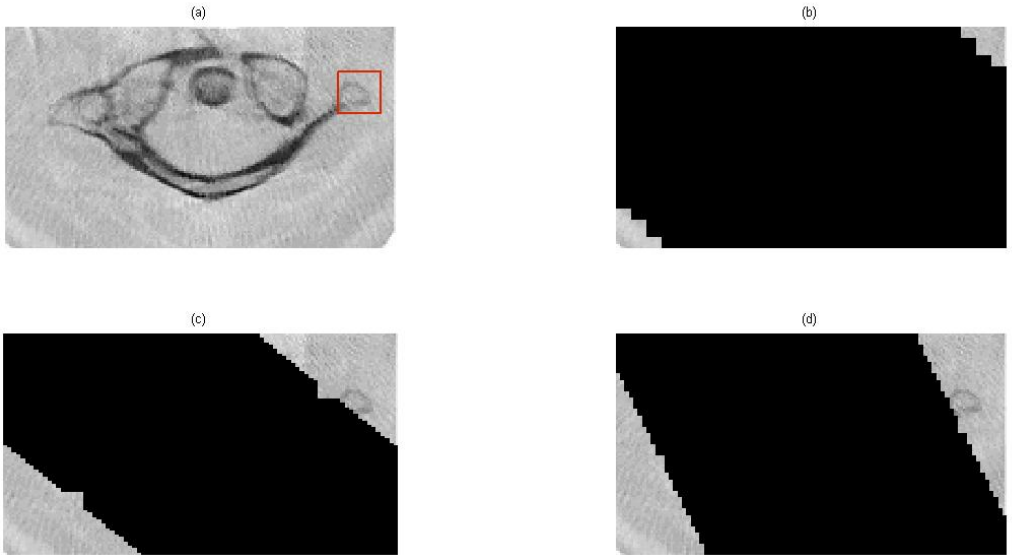

Figure 11: (a) The Atlas phantom (the ROI is the area inside the red rectangle). (b) The ROU for the pair $(-14, 13), (-7, 5)$. (c) The ROU for the pair $(-36, 29), (-26, 21)$. (d) The ROU for the pair $(-22, 45), (-18, 37)$.

As a further perspective, investigation could be carried out in the case of more than two directions. This would allow to enlarge the ROU and, consequently, it would be helpful in studying a wider region of interest. Some results obtained in this paper indeed hold in a more general context, even if a complete generalization seems to require much work.

References

[1] E. Barcucci, A. Del Lungo, M. Nivat, R. Pinzani, *Reconstructing convex polyominoes from horizontal and vertical projections*, Theoretical Computer Science, 155 (1996), pp. 321-347.

[2] E. Barcucci, A. Del Lungo, E. Pergola, R. Pinzani, *ECO: a methodology for the Enumeration of Combinatorial Objects*, Journal of Difference Equations and Applications, 5 (1999), pp. 435-490.

[3] K.J. Batenburg, W. van Aarle, J. Sijbers, *Grey Level Estimation for Discrete Tomography*, in: S. Brlek, C. Reutenauer, and X. Provençal (Eds.): Discrete Geometry for Computer Imagery, LNCS 5810 (2009), pp. 517-529.

[4] S. Brunetti, P. Dulio, C. Peri, *Discrete Tomography determination of bounded lattice sets from four X-rays*, Discrete Applied Mathematics 161 (15) (2013), pp. 2281-2292.

[5] S. Brunetti, P. Dulio, C. Peri, *Discrete Tomography determination of bounded sets in* $\mathbb{Z}^n$, Discrete Applied Mathematics 183 (2015), pp. 20-30.

[6] D.J. De Rosier, A. Klug, *Reconstruction of Three Dimensional Structures from Electron Micrographs*, Nature 217 (1968), no. 5124, pp. 130-134.

[7] P. Dulio, A. Frosini, S.M.C. Pagani, *Uniqueness regions under sets of generic projections in discrete tomography*, in: Barcucci, Frosini, Rinaldi (Eds.), Discrete Geometry for Computer Imagery, LNCS 8868 (2014), pp. 285-296.

[8] I. Dutour, *Grammaires d'objets ènumèration bijections et gènèration alèatoire*, PhD thesis, Thése de l'Universitè de Bordeaux I (1996).

[9] R.J. Gardner, P. Gritzmann, *Discrete tomography: Determination of finite sets by X-rays*, Trans. Amer. Math. Soc. 349 (1997), pp. 2271-2295.

[10] A. Goupy, S.M.C. Pagani, *Probabilistic reconstruction of hv-convex polyominoes from noisy projection data*, Fundamenta Informaticae 135 (2014), pp. 117-134.

[11] L. Hajdu, *Unique reconstruction of bounded sets in discrete tomography*, Electron. Notes Discrete Math., 20 (2005), pp. 15-25.

[12] L. Hajdu, R. Tijdeman, *Algebraic aspects of discrete tomography*, J. reine angew. Math. 534 (2001), pp. 119-128.

[13] G. T. Herman, A. Kuba, *Discrete tomography*, Appl. Numer. Harmon. Anal., Birkhäuser Boston, Boston, MA (1999).

[14] G.T. Herman, A. Kuba (Eds.), *Advances in Discrete Tomography and Its Applications*, Birkhäuser, Boston (2007).

[15] N. Hyvönen, M. Kalke, M. Lassas, H. Setälä, S. Siltanen, *Three-dimensional dental X-ray imaging by combination of panoramic and projection data*, Inverse Problems and Imaging 4 (2010), no. 2, pp. 257-271.

[16] D.E. Knuth, *The Art of Computer Programming, Vol.* 1*: Fundamental Algorithms*, 3rd ed., Addison-Wesley, Longman Publishing Co., Boston (1997) (Exercises 4 and 11, Section 2.2.1).

[17] D.E. Knuth, *The Art of Computer Programming, Vol.* 2*: Seminumerical Algorithms*, 3rd ed., Addison-Wesley Longman Publishing Co., Boston (1997).

[18] J.L. Mueller, S. Siltanen, *Linear and Nonlinear Inverse Problems with Practical Applications*, SIAM, October 2012.

[19] J. Nemeth, *Discrete Tomography with Unknown Intensity Levels Using Higher-Order Statistics*, J. Math. Imaging Vis., to appear (DOI 10.1007/s10851-015-0581-0).

[20] L.T. Niklason et al., *Digital tomosynthesis in breast imaging*, Radiology 205 (1997), no. 2, pp. 399-406.

[21] G. Rozenberg, A. Salomaa (Eds.), *Handbook of Formal Languages, Vol.* 1*: Word, Language, Grammar*, Springer-Verlag, New York (1997).

[22] H.J. Ryser, *Combinatorial properties of matrices of zeros and ones*, Canad. J. Math., 9 (1957), pp. 371-377.

[23] L. Varga, L.G. Nyúl, A. Nagy, P. Balázs, *Local Uncertainty in Binary Tomographic Reconstruction*, Proceedings of the IASTED International Conference on Signal Processing, Pattern Recognition and Applications (2013), Innsbruck, Austria, pp. 490-496.